Materials and Methods

Mice

C57Bl/6 mice were used for all experiments and as wild-type controls unless stated otherwise. B1-8$^{flox/flox}$ mice (a gift from K. Rajewsky) were crossed with the Igκ-deficient Igk-C$^{tm1Cgn/tm1Cgn}$ mice (a gift from J. Langhorne) to produce the B1-8$^{flox/flox}$ Igk-C$^{tm1Cgn/tm1Cgn}$ strain (called B1-8 throughout the manuscript); the strain was backcrossed onto C57Bl/6 background (NIMR internal colony). The majority of B cells in these mice are specific for the nitrophenyl (NP) hapten. Mice were bred and treated in accordance with guidelines set by the UK Home Office and UK NIMR Ethical Review Panel.

B cell purification and cell culture

Primary naïve B cells were obtained from splenocytes following red blood cell lysis (ACK buffer, GIBCO) and negative selection using anti-CD43 microbeads (Miltenyi Biotec). Primary B cells and the Ramos human lymphoma cell line were cultured in RPMI 1640 media (SIGMA) supplemented with 10% fetal bovine serum (Biosera), 1% MEM Non-Essential Amino Acids (GIBCO), 2 mM L-glutamine (PAA Laboratories), 50 μM 2-mercaptoethanol (GIBCO), 100 U/ml Penicillin and 100 μg/ml Streptomycin. Adherent HEK293A, HEK293FT (both from Invitrogen) and PLAT-E cells (a gift from V. Tybulewicz) were cultured in DMEM media (GIBCO) supplemented with 10% FBS, 1% MEM Non-Essential Amino Acids, and 6 mM L-glutamine. 10 μg/ml blasticidin and 1 μg/ml puromycin (both InvivoGen) were added to PLAT-E media, and 0.5 mg/ml Geneticin (GIBCO) was added to HEK293FT media. Suspension HEK293A cells were maintained at 5x10^5 cells/ml, agitated at 120 rpm in Pro293S-CDM (Lonza) supplemented with 1.5% fetal bovine serum and 2 mM L-Glutamine. DCs were differentiated from bone marrow cells using

Flt3 ligand (a gift from G. Stockinger) for 7 days, and matured using LPS for 24 hours. All cells were cultured in incubators humidified with 5% CO_2 at 37°C.

Antigens, antibodies and inhibitors

Antigens

Unless otherwise specified, the antigens were goat $(F_{ab}')_2$ anti-mouse Igκ for primary B cells from C57Bl/6 mice, or goat $(F_{ab}')_2$ anti-human IgM (Southern Biotec) for human Ramos B cells. To generate antigens for the B1-8 B cells, purified, biotinylated, AlexaFluor647-labeled goat $(F_{ab}')_2$ was haptenated with NP or NIP-Osu (Biosearch Technologies). These antigens contained 15 haptens per protein, as determined by absorbance at 430 nm. Cy5 labeling of antigens was carried out using the Monoreactive dye kit (GE Healthcare) and biotinylation was done using EZ-link sulfo-NHS-LC-LC-Biotin (Thermo scientific). For 3D localization of antigen particles, antigen-Qdots were produced by labeling a small number of biotinylated goat $(F_{ab}')_2$ anti-mouse Igκ antigen molecules with a low concentration of streptavidin-conjugated quantum dots (Qdots, Invitrogen). To load cognate immune complexes onto DCs for recognition by B1-8 B cells, we mixed biotinylated NIP-antigen with anti-biotin IgG_1 antibodies (Sigma). For AFM experiments, DCs were loaded with immune-complexes consisting of anti-NP antibodies (Serotec) and NIP-antigens.

Antibodies

Anti-mouse IgM F_{ab} conjugated with Cy5 (Jackson Immunoresearch) was used to stain BCR. Anti-B220-FITC (BD) was used to stain B cell membranes.

Lipid Dyes

To label phospholipid membranes of antigen-presenting substrates, lipophilic carbocyanine dyes, DiI or DiD (both Invitrogen), were incubated with PMS, PLB, PM-PLB or DCs at 2

μM in Hank's balanced salt solution (HBSS) for 10 min at room temperature and washed away.

Inhibitors

Y-27632 (Sigma) and blebbistatin (Caymann Chemical) were incubated with cells in HBSS supplemented with 0.01% BSA. Dynasore (a gift from T. Kirchhausen) was incubated with cells in HBSS with no BSA. All inhibitors were preincubated with cells for 15 min at 37°C before experiments. Unless otherwise stated, blebbistatin and Y-27632 were used at 50 μM, dynasore at 80 μM. Solvent in the appropriate buffer was used as control.

Lentiviral and retroviral infection

Recombinant lentiviruses were produced by lipofectamine-mediated co-transfection of HEK293FT cells with the VSVg and δ8.9 helper plasmids, together with shRNA-containing pLKO.1 plasmids from The RNAi Consortium (TRC) library (Sigma). The shRNA clones were as follows: *Ap2M1* TRCN0000060238 for AP2, *Dnm2* TRCN0000006649 for dynamin2, *Rock1* TRCN0000121093 for Rock1, and *Myh9* TRCN0000029468 for myosin IIa. Empty pLKO.1 was used as control. In independent experiments, the empty pLKO.1 plasmid produced identical results as a pLKO.1 plasmid containing a nonspecific shRNA control. Lentivirus-containing media were harvested 72 hours following transfection and centrifuged with Ramos cells in the presence of 8 μg/ml polybrene (Sigma) for 90 minutes at 1350 x g. Twenty four hours after spinfection, infected cells were selected using 3 μg/ml puromycin.

Retrovirus was produced by lipofectamine-mediated transfection of PLAT-E cells with pMSCV containing one of the following constructs: clathrin light chain-GFP (*29*), LifeAct-GFP (*30*) (a gift from J. Burkhardt), or myosin regulatory light chain (RLC) 12B (MYL12B)-GFP. Primary B cells, pre-stimulated with 1 μg/ml CpG (Sigma) for 24 hours, were

spinfected with retrovirus-containing supernatants in the presence of 20 μg/ml polybrene as above.

Plasma membrane sheets (PMS)

Suspension HEK293A cells were seeded onto poly-l-lysine-coated Labtek imaging chambers (Nunc) and cultured overnight in DMEM to 100% confluency. Cells were then washed in phosphate-buffered saline (PBS) and sonicated with a probe sonicator placed 5 mm above the cells for 20 seconds at room temperature. This shears off the cells, leaving the ventral plasma membrane attached to the coverslip with its cytoplasmic side exposed (*14*, *31*). PMS were blocked with PBS supplemented with 1% BSA and then incubated in HBSS 0.1% BSA with 24 nM biotinylated annexin V (BioVision). After washing, PMS were incubated with 5 μg/ml Streptavidin (Southern Biotec), washed again, and incubated with biotinylated antigens. When not explicitly stated, PMS were loaded with antigens at 1 μg/ml, resulting typically in 50 antigen molecules per μm^2 of the PMS. In some cases, the concentration of antigen was titrated to achieve the density specified in the experiments. The calculation of antigen density on the substrates was performed as previously described (*15*). Briefly, antigen was diluted to a concentration that allowed resolution of single antigen molecules. The average fluorescence intensity of the single antigen molecules was used to convert fluorescence intensity of experimental antigen concentrations to number of antigen molecules per μm^2.

Synthetic planar lipid bilayers (PLB)

1,2-Dioleoyl-*sn*-Glycero-3-Phospho-L-Serine (DOPS) was mixed at a molar ratio of 1:10 with 1,2-dihexanoyl-*sn*-glycero-3-phosphocholine (DOPC, both from Avanti) in choloform, and used to produce planar lipid bilayers as described previously (*15*). Antigen was attached via biotinylated annexin V and streptavidin as described for PMS and its density was quantified as on the PMS.

Planar lipid bilayers from plasma membranes (PM-PLB)

Suspension HEK293A cells were lyzed in 5 mM $NaH_2PO_4/NaHPO_4$, pH 8 at $10x10^6$ cells/ ml for 30 minutes on ice, and then homogenized using Dounce tissue-grinder pestle (Sigma). Nuclei were removed by centrifugation at 500 x g at 4ºC for 10 min and plasma membranes were isolated by centrifugation at 20 000 x g at 4ºC for 30 minutes. The membrane pellet was resuspended in a buffer containing 500 μM $NaH_2PO_4/NaHPO_4$, 100 μM $MgSO_4$, pH 8, on ice for 1 hour. Membrane vesicles were then purified by centrifugation at 100 000 x g at 4ºC. The vesicle pellet was resuspended in the same buffer and used immediately. Vesicles were allowed to settle and rupture on glass coverslips in imaging chambers for 1 hour at room temperature. Antigen was attached via biotinylated annexin V and streptavidin and its density was quantified as on the PMS.

Imaging and image analysis

All microscopy analysis and live-cell imaging was carried out on an Olympus IX81 microscope, with an Andor iXon EMCCD Camera and 100x objective (Olympus). Live-cell imaging was done at 37°C on a heated stage with an objective heater. Total internal reflection fluorescence (TIRF) or epifluorescence timelapse images were acquired with time resolution of 2-5 s for 20 min, and corrected for photo-bleaching. Short, fast imaging of DiI in membrane invaginations was done at 10 frames/s. TIRF angle was setup as shallow as possible to extend the depth of field further away from the coverslip. All images were aligned, background-subtracted and corrected for spectral bleedthrough and photobleaching. Images were analysed using ImageJ and Matlab (Mathworks).

Reconstructed images showing antigen internalization from PMS, PLB and DCs were generated from z-stacks by first deconvoluting the stacks, and then using maximal projection of the middle of the cell along the y axis (PLB and PMS) or z axis (DCs).

Outlines of cells shown in figures were derived from bright-field images.

Quantification of internalization

Internalization of soluble antigens in the presence or absence of the inhibitors was measured using FACS analysis. Cells were incubated with biotinylated goat $F(ab')_2$ anti-mouse Igκ for 30 min on ice, washed and further incubated for 20 min either at 37°C, or on ice. Then, cells were fixed with 2% paraformaldehyde and stained with Cy5-labeled streptavidin. Antigen internalization was calculated by subtracting the streptavidin fluorescence of the heated sample from the cold sample and dividing by the fluorescence of the cold sample.

To quantify internalization of soluble NP and NIP antigens, cells were attached to poly-L-lysine-coated coverslips and incubated with NP or NIP antigens, fixed and stained with Cy3-labeled streptavidin. To determine the intensity of the internalized antigen in each cell, background from regions outside the cells was subtracted. Z-stack images of antigen and streptavidin on cells were processed through a 3D bandpass filter and thresholded to create 3D masks. The antigen mask was applied to the original antigen stack. Next, the streptavidin mask was used to exclude antigen present on the cell surface. The resulting antigen fluorescence was integrated.

Internalization from PMS, PM-PLB and PLB was quantified from z-stack images, similarly as for the soluble antigens, but integrating antigen fluorescence only from image planes above the substrate. Specifically, background was subtracted using regions of interest outside of presenting membranes. Z-stack images of antigen were processed through a 3D bandpass filter and thresholded to create a 3D mask. The antigen mask was applied to the original unfiltered antigen stack to include endosomal antigen and exclude scattered fluorescence background. Internalized antigen fluorescence was then calculated by integrating antigen fluorescence in the masked antigen images in stacks above the substrate. In experiments with

primary cells, we found that all antigen above the substrate was inaccessible to cell-impermeable secondary staining and was therefore considered internalized. In experiments with Ramos B cells, we found that some antigen above the substrate was accessible to secondary streptavidin staining. Therefore, secondary streptavidin staining was used to exclude the streptavidin-colocalized antigen from the analysis as described for soluble antigens. The percentage of internalization was expressed as the intensity of internalized antigen divided by total antigen intensity, which included the internalized antigen and the antigen left on the substrate underneath the cell.

Analysis of membrane invaginations

Membrane invaginations were detected using DiI- or DiD-labeled PMS. The invaginations were equally detectable in epifluorescence illumination and in TIRF. For 3D particle localization, the membrane dyes were excited in epifluorescence mode. For timelapse TIRF imaging, we used p-polarized laser, which produces evanescent field that is mostly vertically polarized and excites therefore preferentially DiI dyes in vertically oriented membranes (*32*, *33*).

Membrane invaginations were tracked in space and time from timelapse images of DiI or DiD stained PMS using previously developed tracking algorithms (*15*). Briefly, image sequences were aligned and normalized to the image of the PMS prior to cell spreading, and then processed using a bandpass filter. Fluorescent spots were tracked and their lifetime was calculated from the length of the tracks.

Intensity of the antigen, myosin IIa RLC-GFP or LifeAct-GFP associated with the invaginations was calculated as the mean intensity in 5 by 5 pixel regions centered on the track coordinates, including 1 to 3 frames before the start and 1 to 2 frames after the end of the track. For antigen, the intensities were normalized to the average antigen intensity on the

PMS before cell spreading. For myosin RLC-GFP and LifeAct-GFP, the intensities were normalized to the average intensity in the synapse in the same frame.

Calculation of the colocalization of invaginations with CCSs was performed in primary B cell blasts infected with retroviruses containing clathrin light chain-GFP (*29*). Positions of CCSs were first detected using the tracking algorithms described above. Colocalization for each time point in each invagination lifetime was considered positive if there was a CCS within 2 pixels of the invagination coordinates. Control colocalization in each cell was performed using CCSs shifted by 5 pixels in a random direction, maintaining boundary conditions within the cell.

3D particle localization

DiI-labeled PMS were loaded with biotinylated antigen and a small fraction of the antigen on the PMS was subsequently labeled with streptavidin-conjugated Qdots (Invitrogen). Imaging was performed in epifluorescence mode. 3D localization of the Qdots was performed using a cylindrical lens (f = 1 m) inserted into the infinity space of the emission path (*34*). Gaussian fitting was used to extract the elipticity of the fluorescent spots. To convert the data to vertical distances, we acquired calibration images of Qdots attached to coverslips, while stepping up the microscope z-stage in 10 nm increments. Positional accuracy was estimated from timelapse images of stationary Qdots on coverslips and was ~40 nm. Vertical position of the Qdots in B cell synapses were expressed as their vertical distance from the mean position of Qdots present on the coverslip outside of synapses.

Fluorescence recovery after photobleaching (FRAP)

FRAP imaging was performed using TIRF microscopy at 37°C. Membranes were imaged for 10 seconds, and then a circular region of 13 μm in diameter was bleached at maximum laser power for 1 minute using the field diaphragm. Membranes were then imaged every 10

seconds for an additional 10 minutes. Fluorescence recovery was analyzed by measuring antigen or DiI intensity in the FRAP region throughout the experiment. The intensity in the FRAP region was normalized to fluorescence in a non-bleached control region.

B1-8 F_{ab} production and bio-layer interferometry binding measurements

B1-8 F_{ab} was produced in suspension culture of HEK293A cells co-transfected with constructs containing the B1-8 heavy chain with a six-histidine tag and the λ_1 light chain. The B1-8 F_{ab} was purified from culture supernatants using affinity chromatography followed by gel filtration. Binding measurements were performed with Octet (Fortebio) using biotinylated NP- or NIP-antigen attached to streptavidin-functionalized chips and 0.2-2 μM soluble B1-8 F_{ab}. Association rate, dissociation rate and affinity were determined from fitting of kinetic models to the data.

AFM force spectroscopy

AFM was performed using a setup integrating AFM and optical imaging (JPK instruments). To carry out force spectroscopy with PMS, PLB, PM-PLB and DCs, gold-coated Biolever cantilevers (nominal spring constant 6 mN/m, Olympus) were exposed to UV light for 30 min and then conjugated to DOTP (Pierce)-activated streptavidin. The cantilevers were then washed and used immediately. Spring constant was measured for each tip using the JPK software and varied between 5.2 and 6.0 mN/m. PMS, PLB and PM-PLB were loaded with biotinylated antigens as described above. Mature bone marrow-derived DCs were loaded with immune-complexes consisting of anti-NP antibodies (Serotec) and NIP-antigens for 1h on ice. The cells were washed and attached to poly-L-lysine coated coverslips. Force spectroscopy was carried out on PMS, PLB or PM-PLB visualized using DiI, and on the dorsal surfaces of the DCs' lamellopodia, visualized by brightfield imaging. Negligible binding was observed in samples lacking the annexinV-biotin or antigen.

To measure rupture forces between antigens and the B1-8 F_{ab} or the B1-8 BCR, the Biolevers were conjugated to NP or NIP antigen reduced with 2 mM TCEP. B1-8 F_{ab} fragment was activated with EDC/sulfo-NHS (Pierce) and attached to N-(2-aminoethyl)-3-aminopropyltrimethoxysilane (Sigma)-treated coverslips. Purified primary B1-8 B cells were captured on poly-L-lysine coated coverslips and force measurements were carried out on the dorsal surfaces of their lamellopodia. The overall frequency of binding of the cantilever to the B1-8 F_{ab} was 16.3% and 20.6% for the NP and NIP antigens, respectively, compared to 7.6% and 7.2% for the control surface lacking the B1-8 F_{ab}. The frequency of binding to the B1-8 cells was 19.5% and 24.3% for the NP and NIP antigens, respectively, compared to 6.5% and 4.3% for binding to control cells from C57Bl/6 mice. Tip retraction speeds were from 0.1 to 50 μm/s to give various rates of force increase (bond-loading rates). Data were processed using the JPK analysis software. Rupture forces and rupture distances were measured from force versus tip-sample separation curves containing single-step ruptures (Fig. S7A, left). The force histograms of the controls were subtracted from the histograms obtained with the B1-8 F_{ab} or the B1-8 BCR and matched for the number of tip approaches. Mean rupture forces were obtained from gaussian fitting of the resulting rupture force histograms. Loading rates were calculated from the slope of a line connecting the origin and the rupture point of the force versus time curves (Fig. S7A, right). For the BCR-antigen bonds, we also measured the rupture distances, which rose monotonically with tip retraction speeds (Fig. S7C). This argues that the forces measured on B cell surfaces are not affected by different elasticity of the B cell membranes under different tip retraction speeds.

Plots of mean rupture forces versus loading rates for antigen-antibody bonds were fitted with Bell's formula (*24*):

$$F(R) = \frac{k_B T}{x_b} \ln\left(\frac{R x_b}{k_{off} k_B T}\right),$$

where F(R) is the mean rupture force at loading rate R, k_B is the Boltzmann constant, T is temperature, and x_b is the barrier distance.

Rupture force data for the BCR-antigen could not be fitted with Bell's formula or with other models (*35*, *36*) without dramatically altering binding parameters. Conversion of rupture force distribution to bond half-lives at the mean force was performed using the following formula (*23*):

$$t\left(\langle F\rangle\right)=\frac{\sqrt{\frac{\pi}{2}\left(\langle F^2\rangle-\langle F\rangle^2\right)}}{R\left(\langle F\rangle\right)},$$

where t(⟨F⟩) is the half-life at the mean force F, F are the rupture forces and R(⟨F⟩) is the mean loading rate.

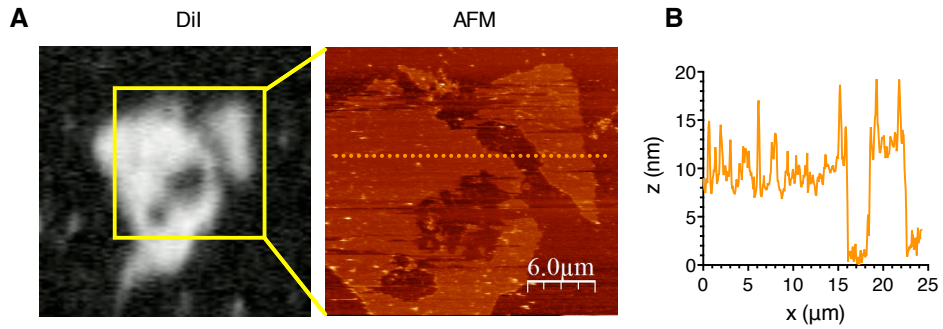

Fig. S1. Atomic force microscopy (AFM) imaging of PMS. (**A**) Left, fluorescent image of PMS labeled with the hydrophobic dye, DiI, on a coverslip. The area indicated by the yellow rectangle was scanned by AFM (right). (**B**) Vertical profile of the dotted line indicated in (A).

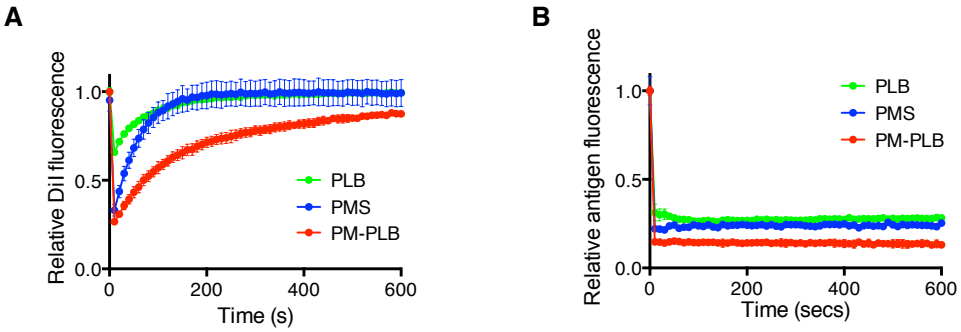

Fig. S2. Measurements of lipid and antigen diffusion in membrane substrates using fluorescence recovery after photobleaching (FRAP). (**A**) FRAP of hydrophobic dye, DiI, shows high mobile fraction, indicating fluidity and continuity of all substrates. Diffusion was fastest in PLB and slowest in PM-PLB. (**B**) Antigen (anti-Igκ) anchored to the membranes shows low mobility, similar in all substrates.

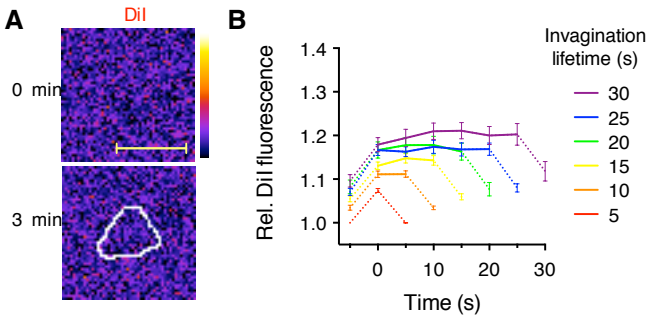

Fig. S3. Formation of membrane invaginations in B cell synapses. (**A**) Control for Fig. 2A showing no changes in DiI fluorescence under a primary B cell (white outline) in the absence of antigen on the PMS. (**B**) Normalized DiI fluorescence in tracked membrane invaginations of the indicated lifetimes from the same dataset as in Fig. 2F. Dotted lines show fluorescence at the invagination site before and after the invagination lifetime.

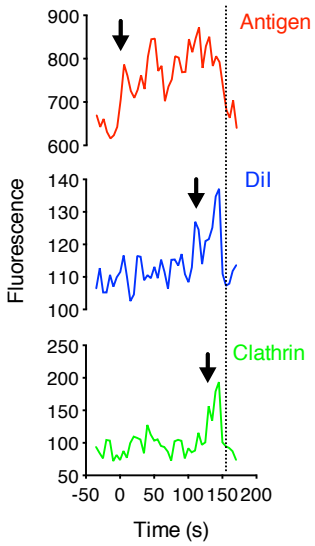

Fig. S4. Primary B cell antigen extraction by CCS-mediated pinching off of membrane invaginations. Fluorescent traces of antigen, DiI and clathrin-GFP in a single antigen microcluster shows sequential formation of the antigen microcluster, invagination of the membrane, and recruitment of clathrin (arrows). All three signals disappear simultaneously (dotted line), indicating internalization.

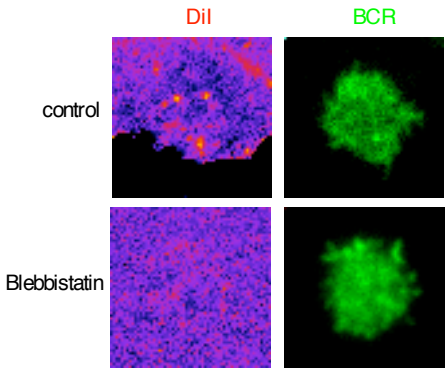

Fig. S5 . Primary B cell spreading on antigen-loaded PMS in the presence or absence of the myosin IIa inhibitor, blebbistatin.

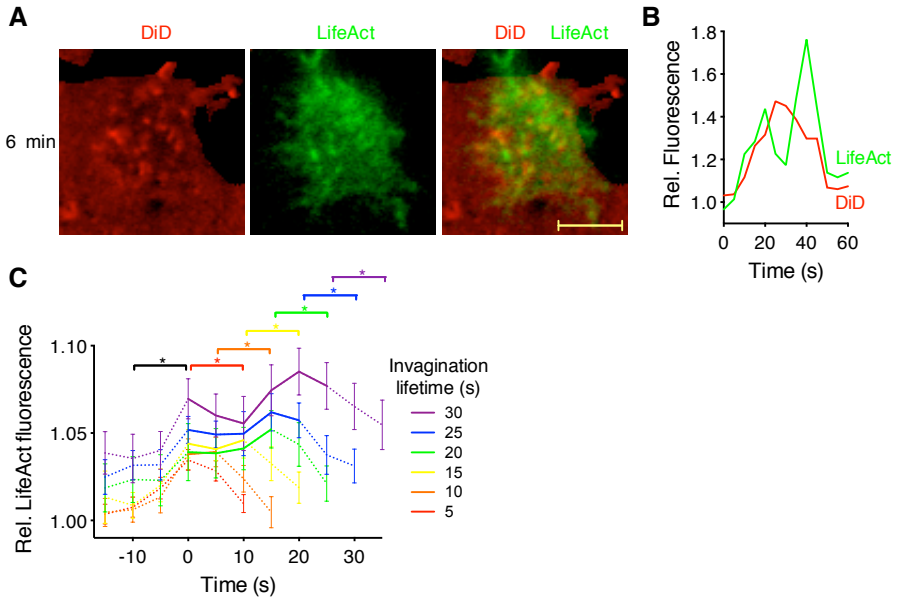

Fig. S6. Localization of F-actin in B cell synapses as reported by the LifeAct-GFP probe. (**A**) TIRF image of a primary B cell expressing LifeAct-GFP (green) spread on PMS labeled with DiD (red) and loaded with antigen. (**B**) Fluorescent intensities in a single invagination showing two waves of LifeAct recruitment. (**C**) Quantification of LifeAct fluorescence in membrane invaginations grouped by lifetime. Dotted lines show fluorescence at the invagination site before and after the invagination lifetime. (mean±SEM, n=13 cells). *, $p<0.015$ in paired t-tests. Scale bars, 5 µm.

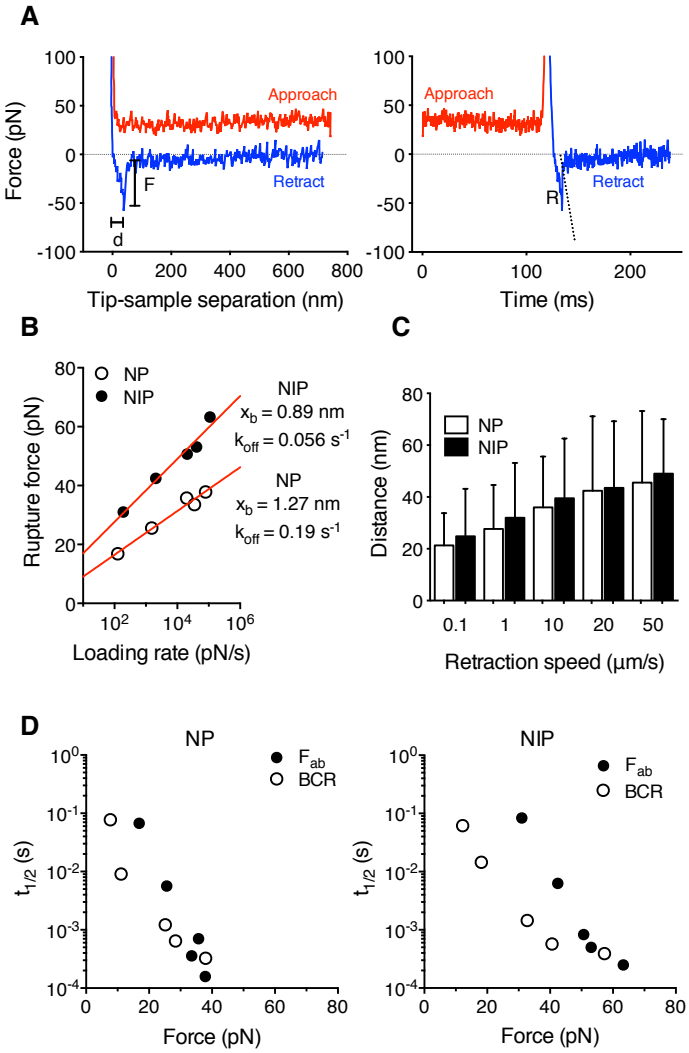

Fig. S7. Force spectroscopy with the B1-8 F_{ab} and BCR. (**A**) An example of the approach and retraction curves using NIP-conjugated cantilever and a B1-8 B cell. Speed of cantilever movement was 10 μm/s. Plots of force versus tip-sample separation (left) and force versus time (right) show measurements of rupture force (F), rupture distance (d) and loading rate (R, slope of the indicated line). (**B**) Fitting of Bell's equation (see Materials and Methods) to force spectroscopy data for the B1-8 F_{ab} on coverslips. (**C**) Rupture distances between the antigen-conjugated AFM cantilevers and the BCRs on B1-8 cell surfaces for the indicated retraction speeds. (**D**) Plot showing the decrease of B1-8 bond half-life with force. Half-lives of B1-8 bonds were calculated from rupture force histograms (see Materials and Methods).

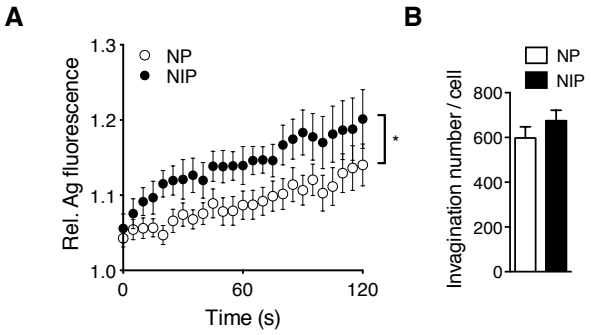

Fig. S8. Quantification of antigen microcluster growth and the number of invaginations in synapses of B1-8 B cells with NP or NIP antigens. (**A**) Antigen microclusters were tracked during synapse formation between B1-8 B cells and PMS loaded with NP or NIP antigens. Intensities were normalized to average antigen fluorescence on the PMS before B cell spreading. Data are mean±SEM of n=9 individual cells. Datasets were significantly different between the antigens in two-way ANOVA, $p<0.001$. (**B**) Number of invaginations. Data are mean±SEM of individual cells from same experiments as in Fig. 4F, G.

	k_{on} ($\mu M s^{-1}$)	K_{off} (s^{-1})	K_d (μM)
NP	**0.27 ± 0.02**	**0.60 ± 0.03**	**2.2 ± 0. 2**
NIP	**0.25 ± 0.01**	**0.08 ± 0.01**	**0.33 ± 0.05**

Table S1. Kinetic parameters of the soluble monovalent F_{ab} fragment from the B1-8 antibody binding to NP and NIP antigens determined by bio-layer interferometry.

Movie S1. TIRF timelapse showing primary B cells labeled with anti-IgM F_{ab} (red) spreading and extracting antigen (anti-Igκ, green) from PMS. Disappearance of antigen from the TIRF view indicates internalization. Elapsed time is shown in minutes and seconds.

Movie S2. TIRF timelapse showing a primary B cell labeled with anti-IgM F_{ab} (green, right panel) spreading onto antigen (anti-Igκ)-loaded PMS with incorporated DiI (fire color scale, left panel). DiI intensity was normalized to the DiI image before B cell spreading. Elapsed time is shown in minutes and seconds.

Movie S3. TIRF timelapse showing membrane invagination of DiI-labeled PMS (fire scale, left panel) and antigen (anti-Igκ) clustering (green, right panel) in a primary B cell synapse. Antigen disappearance indicates internalization. DiI intensity was normalized to the DiI image before B cell spreading. Elapsed time is shown in minutes and seconds.

Movie S4. TIRF timelapse showing a primary B cell expressing myosin IIa RLC-GFP (green) during spreading on DiD-labeled PMS (red) loaded with antigen (anti-Igκ). DiD intensity was normalized to the DiD image before B cell spreading. Elapsed time is shown in minutes and seconds.

Movie S5. TIRF timelapse showing a B cell expressing Lifeact-GFP (green) during spreading on DiD-labeled PMS (red) loaded with antigen (anti-Igκ). DiD intensity was normalized to the DiD image before B cell spreading. Elapsed time is shown in minutes and seconds.